Multi-scale flow estimation within stereoscopic PIV processing based on deep learning

L. Hristozova[1*], M. Klaas[1], W. Schröder[1]

1: Chair of Fluid Mechanics and Institute of Aerodynamics, RWTH Aachen University, Aachen, Germany
*Corresponding author: L.Hristozova@aia.rwth-aachen.de

Keywords: PIV processing, Stereoscopic PIV, Deep learning, Optical flow.

ABSTRACT

Classical methods of particle-image velocimetry (PIV) based on state-of-the-art cross-correlation algorithms constitute a spatial filtering operation that leads to a loss of spatial resolution of the estimated velocity fields. This is associated with numerous limitations, e.g., when it comes to aligning high-fidelity numerical simulations, since the detection of small turbulent scales is often precluded. An optical flow neural network adapted for PIV processing, called RAFT-PIV, can overcome the drawback of reduced spatial resolution while maintaining the reliability and robustness of the classical approach. The present work aims to extend the application of the aforementioned deep learning based method by integrating it within a stereoscopic PIV processing workflow. Experimental data from an optically accessible single-cylinder combustion engine the flow field of which is characterized by complex, three-dimensional flow structures and a broad range turbulent scales are processed using RAFT-PIV. The 2D-3C vector fields obtained from stereoscopic reconstruction are compared against a classical cross-correlation based PIV evaluation, providing insight into instantaneous quantities and turbulent structures. A qualitative comparison of the instantaneous in-plane and out-of-plane velocity components reveals that the reconstructed flow obtained from the deep learning based estimation includes a wide range of resolved turbulent length scales. It outperforms the classical method. Furthermore, the findings of the present study demonstrate that the pixel accuracy has an effect on both physical quantities and turbulence characteristics. In particular, an increase in turbulent kinetic energy is observed across the engine cycles of the investigated engine flow states. Moreover, a higher fraction of three-dimensional isotropic turbulent structures is derived from RAFT-PIV compared to the results from the cross-correlation based technique.

1. Introduction

Particle-image velocimetry (PIV) is one of the most versatile and widely established state-of-the-art non-intrusive flow measurement techniques to extract flow velocity data in gaseous or liquid media. Due to its convenient scalability and associated potential to acquire spatial information on all three components of the velocity vector with a single measurement, PIV has become one

of the most important tools in both low-speed and high-speed applications. Despite various advantages such as its high robustness and moderate computing time, cross-correlation (CC) based reconstruction of the velocity field is also associated with several downsides. One of the typically encountered drawbacks of the classical approach is an inherent limitation of spatial and in some cases, also the temporal resolution which usually depends on the available measurement system. Since cross-correlation inherently works as a spatial filter, it effectively reduces the usable resolution, which typically makes comparisons with high-fidelity numerical simulations challenging. Hence, it might happen that small-scale structures are not captured due to the sparse spatial resolution, which impairs the comprehensive analysis of the interaction between multi-scale vortices in highly turbulent flows.

Even though advances in camera technology over the past decades were able to partially overcome the general trade-off between spatial and temporal resolution, i.e., allowing for high-speed acquisition at megapixel resolutions, cross-correlation based methods still constitute a limiting factor. Determined by the desired and computationally affordable size of the interrogation window, a drastic downsampling of the inherent image resolution still prevails.

This is where deep learning (DL) methods come into play since they are usually not subject to such limitations. In particular, a neural network optical flow estimator called RAFT-PIV introduced by Lagemann et al. (2021) is capable of pixelwise accurate flow prediction. This method promises to overcome disadvantages of the conventional approach, i.e., enabling a spatially more detailed investigation while using the identical input data, i.e., particle images. Providing access to structures and phenomena previously precluded due to their size will further open up new possibilities in synergetic use and more precise alignment of numerical simulations and experiments. In particular, resolving small turbulent scales also in experiments is essential to thoroughly validate high-fidelity numerical simulations. Therefore, the scope of this study is to extend the range of applications of the novel neural network RAFT-PIV to its use within the stereoscopic PIV image processing workflow.

2. Methods

The workflow of stereoscopic PIV image processing involves three main steps: (1) a calibration procedure, in which the object-space mapping function and the viewing direction of each camera are determined; (2) image processing, i.e., evaluating the particle displacement from PIV images; (3) three-dimensional flow reconstruction, computing the real flow velocity field based on the position of both cameras. In this work, we perform the calibration procedure in step (1) and pass the dewarped images to step (2), where we evaluate the images once with a deep learning based algorithm and once with a cross-correlation based algorithm. In step (3), we reconstruct the flow fields obtained by each method based on the camera orientation determined in step (1). The methods

used to estimate the flow fields of each camera are presented in this section. Detailed descriptions of the procedures involved in steps (1) and (3) within the stereoscopic PIV workflow, as well as classical PIV processing, can be found in Raffel et al. (2018).

The DL method used to predict the two-dimensional particle displacement for each camera in step (2) is an optical flow neural network based on the Recurrent All-Pairs Field Transforms (RAFT) architecture by Teed & Deng (2020) and adapted for PIV processing by Lagemann et al. (2021), called RAFT-PIV. The network operates on image input resolution and is capable of predicting flow fields with pixelwise spatial resolution. Extensive validation (Lagemann et al., 2021, 2022) demonstrated that RAFT-PIV outperforms current neural networks for PIV and matches the accuracy of state-of-the-art algorithms. Extending the model with a Global Motion Aggregation (GMA) module, similar to the work of Jiang et al. (2021), further improves the precision of the predicted flow by reducing outliers caused by occluded regions or out-of-plane motion. To be able to estimate the particle displacement even under poor image conditions and under highly three-dimensional flow, the RAFT-PIV approach extended with the GMA module is applied in the present work.

The image processing with RAFT-PIV can be briefly described as follows. Firstly, the most relevant image patterns of each image in a pair are extracted through convolutional operations, then the similarities of these patterns are computed based on all-pairs correlation, and finally, the flow is iteratively predicted through a convolutional gated recurrent unit. The network is trained on synthetic PIV images of size $128 \times 128 \mathrm{px}^2$ generated from DNS data that include key flow phenomena and contain realistic image conditions typical for PIV images. Detailed information on the training data and network architecture adapted for PIV processing can be found in Lagemann et al. (2021).

To provide a benchmark for the deep learning approach, the PIV data are evaluated with a cross-correlation based in-house code (Marquardt et al., 2019). The PIV images are processed using a multi-grid approach with interrogation window size of 32 px $\times$ 32 px with 75% overlap, resulting in an 8px vector spacing, i.e., a reduction in the input resolution by a factor of eight. A normalized median test is used to identify outliers in the displacement fields.

3. Experimental Data

The performance of the present optical neural flow network is investigated by applying the two methods described above to PIV measurements of a single-cylinder engine flow. The measurements of the flow field in an optical research engine with direct-injection spark-igniton (DISI) are conducted in a high-speed stereoscopic PIV (HS-PIV) setup at the Institute of Aerodynamics, RWTH Aachen University, by Braun et al. (2020). Characteristics of the engine and operating parameters are listed in Table 1.

Table 1. DISI engine and operating parameters adapted from Braun et al. (2020).

Engine parameter	Value
Bore	75 mm
Stroke	82.5 mm
Displacement volume	364 cm^3
Compression ratio	7.4:1
Number of valves	4
Valve lift	9 mm
Intake valve diameter	27.1 mm
Exhaust valve diameter	23 mm
Intake valves open (1 mm lift)	12° atdc
Intake valves close (1 mm lift)	196°atdc
Exh. valves open (1 mm lift)	204°btdc
Exh. valves close (1 mm lift)	20°btdc
Connecting rod length	146 mm
Crank radius	42.2 mm
Oil temperature	≈60°C
Intake temperature	≈20°C
Intake pressure	100kPa
Engine speed	1,500 rpm
Tumble number	≈2-4

The HS-PIV measurements are conducted by illuminating a thin light sheet (approx. 1 mm) in the tumble plane using a high-speed double-cavity PIV laser (Darwin Duo 527-100 M) with a wavelength of 527 nm. DEHS particles with mean diameter of approx. 0.35-0.45 μm are used as seeding. The stereoscopic setup includes two pco.dimax HS4 cameras with Tamron 180 mm macro lenses with a focal length of f/5.6. The cameras are arranged at an $\pm 45^\circ$ angle to the tumble plane in Scheimpflug condition. More details on the research engine and on the experimental setup can be found in Braun et al. (2020, 2019).

4. Results

Two piston positions, i.e., one at bottom dead center at a crank angle (CA) of 180° and one at mid-compression at CA of 270°, with nearly two hundred engine cycles for each crank angle are processed using RAFT-PIV, and the in-house cross-correlation based method. The results obtained with both methods are first compared in terms of spatial resolution, followed by the effect of the

resolution on various kinetic energy terms and on the characteristics of the involved turbulence.

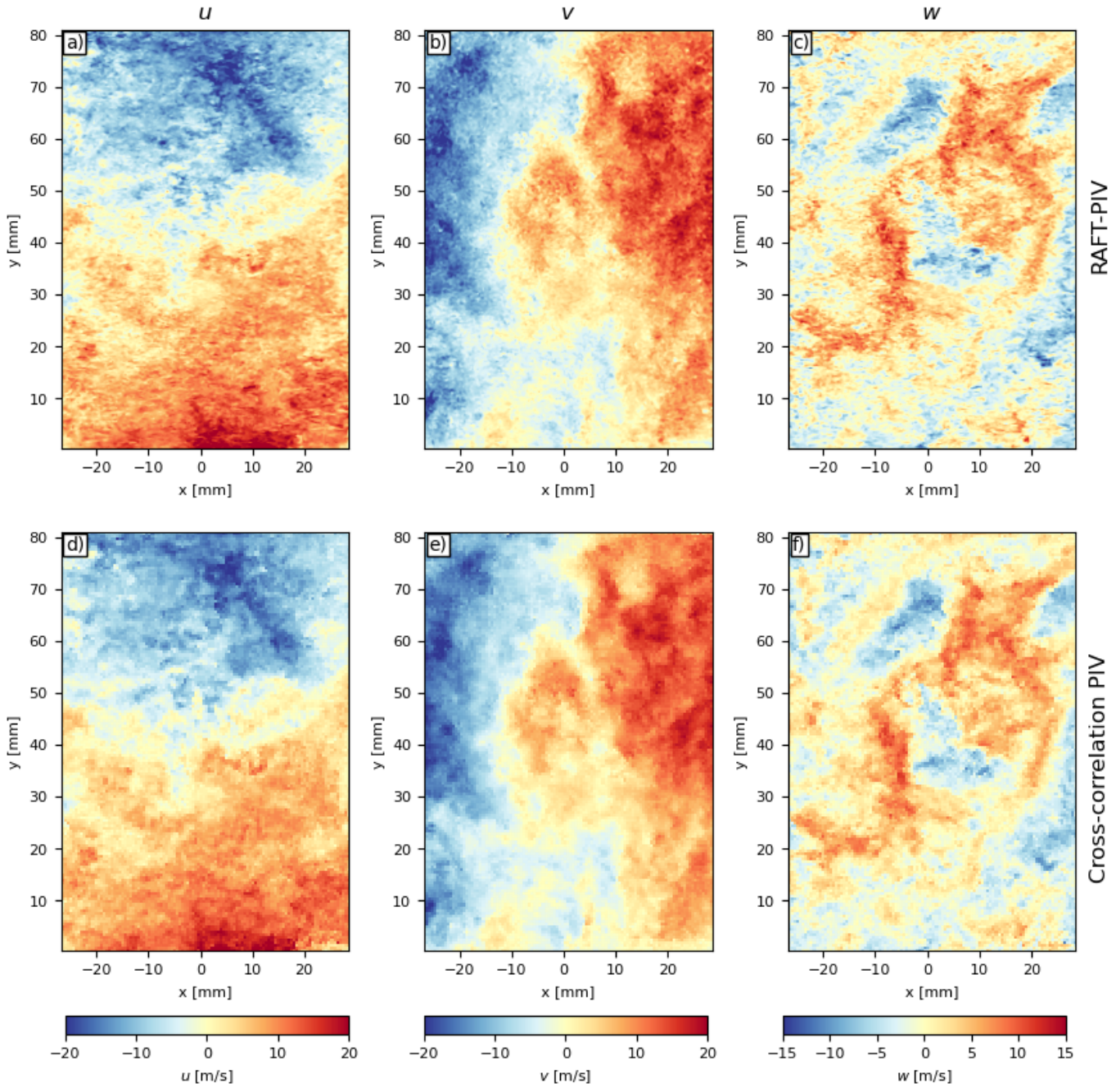

Figure 1. Instantaneous velocity components u (a,d), v (b,e), w (c,f) of the reconstructed flow for the fifth engine cycle at a crank angle of 180° obtained from PIV processing using RAFT-PIV (a-c) and cross-correlation PIV (d-f).

The three instantaneous velocity components $\vec{v} = (u, v, w)^T$ obtained after flow reconstruction are separated into an ensemble-averaged mean part $\overline{u}$ and a fluctuating part u' based on the Reynolds decomposition $u = \overline{u} + u'$. The mean velocity is determined based on N cycles for each CA, where

N=198, while u' as well as further derived parameters based on u' include both cyclic variations and turbulent fluctuations.

Figure 1 shows the results of the instantaneous in-plane velocity components u and v as well as the out-of-plane velocity component w of the reconstructed flow. For brevity, the results focus one engine cycle (n=5) at a crank angle of 180°. The comparison of the estimated flow obtained from PIV processing with RAFT-PIV (Figure 1 (a-c)) and cross-correlation based PIV (Figure 1 (d-f)) shows that the DL-based method is able to accurately predict the particle displacement of each camera such that equivalent results of the three instantaneous velocity components are achieved by both methods. The pixel accuracy of the flow estimation, however, allows the resolution of a wide range of turbulent length scales. In particular, captured with the limited spatial resolution of the benchmark algorithm, substantially smaller structures are sharply resolved by the present approach. The finer resolution of the results indicates that more detailed information can be obtained since flow structures with a more defined shape and length are identified locally.

A crucial parameter characterizing the dynamics within an engine flow, which in turn is related to the engine efficiency, is the kinetic energy. Therefore, the impact of the enhanced spatial resolution on this parameter is analyzed next. The total kinetic energy E_{tot} is examined based on the instantaneous flow and the turbulent kinetic energy K determined by the velocity fluctuation according to $E_{tot} = \frac{1}{2}(u^2 + v^2 + w^2)$ and $K = \frac{1}{2}((u')^2 + (v')^2 + (w')^2)$.

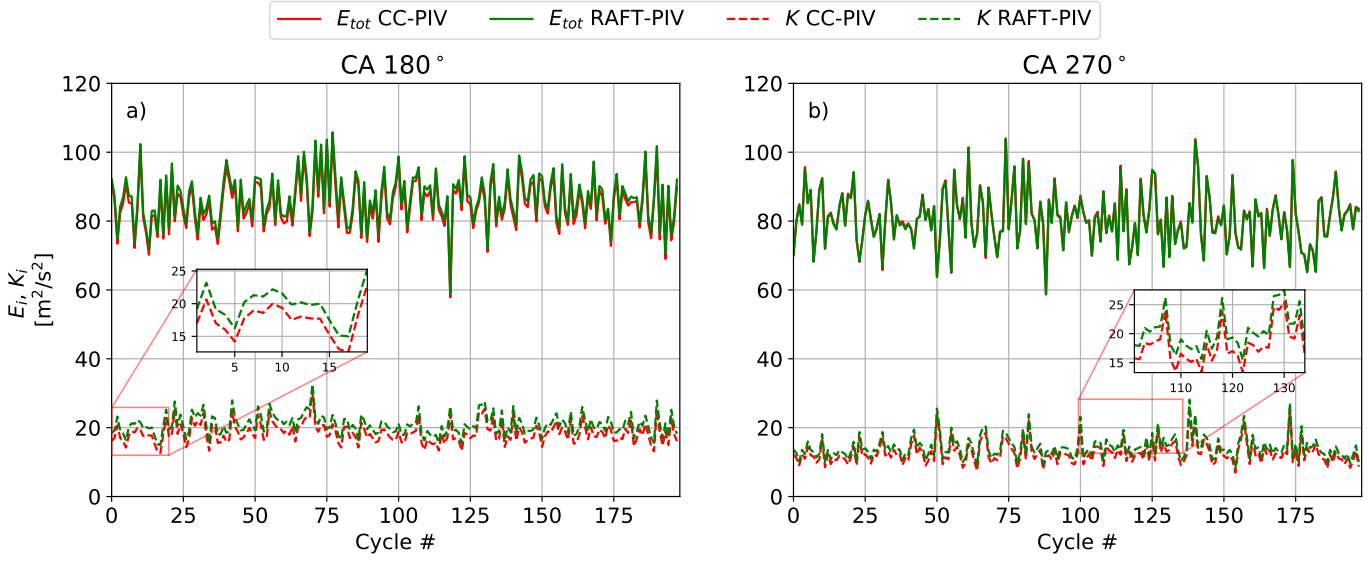

Figure 2. Plane-averaged total and turbulent kinetic energy distribution over N engine cycles for crank angles a) CA=180° and b) CA=270° evaluated with RAFT-PIV and cross-correlation based PIV (CC-PIV).

The plane-averaged total and turbulent kinetic energy for N engine cycles at a crank angles of CA=180° and CA=270° are shown in Figures 2 (a) and (b). Overall, the distribution of both energy

terms reveals a comparable trend for both PIV processing methods, which is consistent with the observations in Braun et al. (2020). A significant increase in turbulent kinetic energy (dashed lines), present in both evaluated engine states, results from the improved spatial resolution with RAFT-PIV. The offset varies between 7% and 21% for different cycles and is on average around 13% across all N samples. As for the total kinetic energy E_{tot}, we observe a slight increase of about 2% at CA=180°, whereas the distribution obtained by both PIV methods virtually coincides during compression (Figure 2 (b)).

Providing more accurate data for a more detailed understanding is a key motivation for achieving higher spatial resolution. Since classical PIV evaluation methods are able to spatially resolve the flow field up to a certain fraction of the original camera resolution that strongly depends on the interrogation window size, the influence of the finer spatial resolution on the turbulence characteristics gained by using RAFT-PIV is analyzed next.

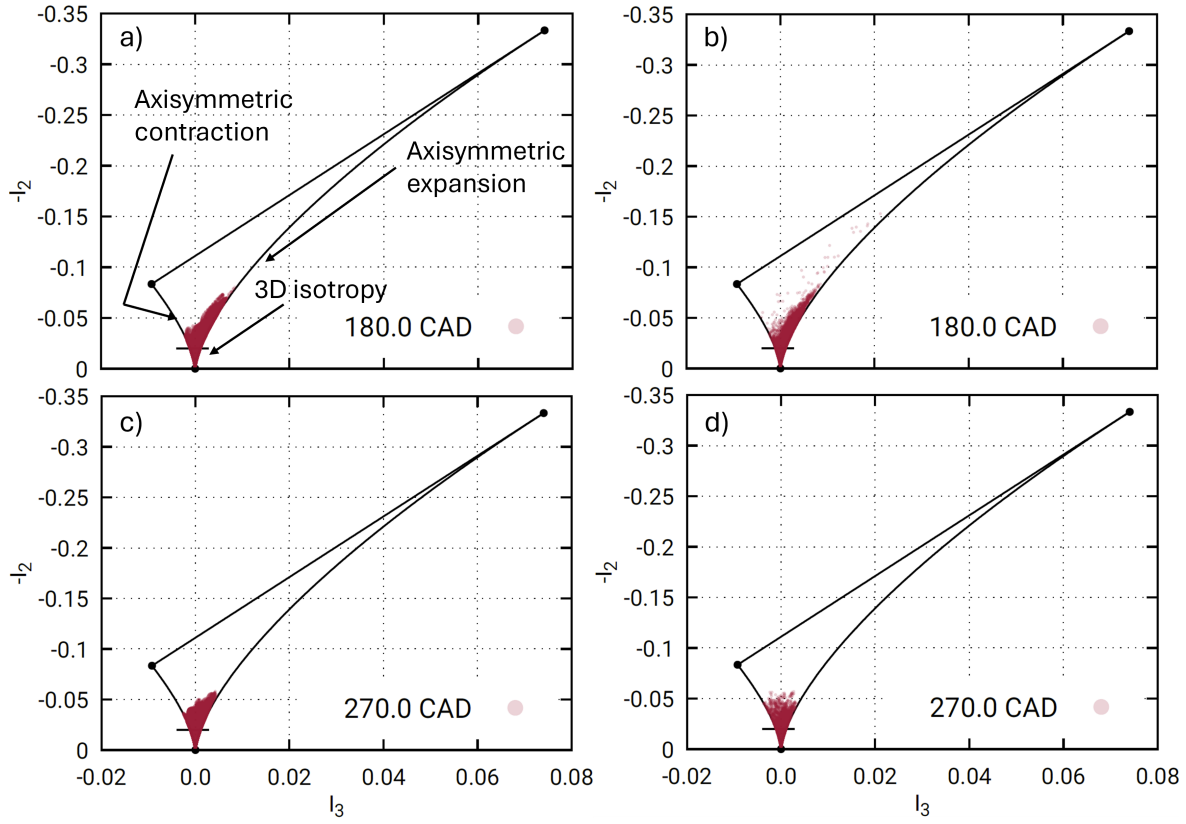

Figure 3. Characterization of turbulence state with anisotropic invariant map according to Lumley & Newman (1977) at CA=180° (a,b) and at CA=270° (c,d) for RAFT-PIV data (a,c) and CC-PIV data (b,d).

The turbulence state using the anisotropic invariant map or Lumley triangle according to Lumley & Newman (1977); Choi & Lumley (2001) is examined. The distribution of the second and third invariants of the Reynolds stress tensor for both evaluated engine flow states is shown in Figure 3. According to Choi & Lumley (2001), the location of the invariants in specific regions within

the Lumley triangle is related to turbulence with different characteristics. Data scattered in the direction of the edges of the turbulence triangle is associated with isotropic turbulence, with three-dimensional isotropy located at the origin of the triangle (see annotation in Figure 3 (a)). Invariants along the left and right boundaries with respect to the origin indicate axisymmetric turbulence. In the case of contraction (left boundary), one component of the turbulent kinetic energy is smaller, resulting in turbulent eddies stretched in the axial direction, while along the right boundary (expansion), one component is larger and the eddies are considered to not have a distinct shape or direction (Choi & Lumley, 2001).

Figures 3 (a) and (b) show the distribution of the invariants for crank angle 180°. The results obtained by RAFT-PIV are plotted in (a) and those with cross-correlation based PIV method in (b). In both cases, the data are mostly scattered toward the triangle origin, indicating the presence of 3D isotropic turbulence and along the axisymmetric expansion boundary. Only a small fraction of the points are associated with the state of axisymmetric contraction. The differences between the two methods are evident in the amount of data distributed in the above-mentioned regions. In the case of DL flow prediction, 10% more data with second invariant below a threshold of 0.02 ($-I_2 < 0.02$) are found, while the amount of axisymmetric turbulence decreases. This is approx. 8% in the expansion and 2% in the contraction state. Furthermore, for the flow estimated using the classical method, it can be observed that individual data points spread towards the center of the Lumley triangle, which is not the case for the results shown in Figure 3 (a).

The flow during compression (CA=270°) (Figures 3 (c) and 3 (d)) is characterized mostly by three-dimensional isotropic turbulence, since more than 70% of the data is located in the region of 3D isotropy with ($-I_2 < 0.02$). This behavior is seen for the flow evaluated by RAFT-PIV (Figure 3 (c)) as well as for the flow evaluated with the classical PIV method (Figure 3 (d)). The differences between the two flow estimation approaches are similar to the results presented for a crank angle of CA=180°. With finer spatial resolution, about 11% more data points are identified as 3D isotropic turbulence, while the detected axisymmetric turbulence is reduced by 5% and 6% for the expansion and the contraction states.

5. Conclusions

A deep learning based method for PIV estimation is used within the stereoscopic PIV image processing workflow. To estimate the particle displacement of each camera in a stereoscopic PIV measurement, the conventional cross-correlation based method is replaced by a well-proven neural network approach for PIV application, called RAFT-PIV. The performance of the network is investigated applying the method to experimental PIV data of a single-cylinder engine flow measured by high-speed stereoscopic PIV. As a benchmark for the predicted flow fields, the flow is also analyzed using a cross-correlation based algorithm. The aim of this work is to extend the application

of RAFT-PIV and to investigate the influence of spatial resolution on physical quantities as well as turbulence characteristics derived from 2D-3C velocity fields.

The analysis of the instantaneous velocity fields shows that the current deep learning based approach is able to compete with a standard PIV estimation method when applied within a stereoscopic PIV processing workflow. The significantly enhanced spatial resolution resulting from per-pixel flow prediction overcomes the limitations of classical methods, flow structures of both large and small turbulent scales can be resolved. As a consequence, turbulent structures of significantly smaller scale were sharply resolved and more detailed information can be extracted from the estimated flow fields.

The analysis of the physical quantities derived from the predicted velocity fields revealed an increase in turbulent kinetic energy within both investigated engine flow states. In addition, the investigation of the turbulence characteristics showed a 10% greater amount of three-dimensional isotropic turbulent eddies for the increased spatial resolution.

Acknowledgements

This research was funded by the Deutsche Forschungsgemeinschaft within the research project 'Learning Deep Optical Flow Estimation for Particle-Image Velocimetry' (DFG SCHR 309/79). The authors gratefully acknowledge the Gauss Centre for Supercomputing e.V. (www.gauss-centre.eu) for funding this project by providing computing time on the GCS Supercomputer JUWELS at Jülich Supercomputing Centre (2021).

References

Braun, M., Klaas, M., & Schröder, W. (2020). Analysis of cyclic variation using time-resolved tomographic particle-image velocimetry. *SAE International Journal of Advances and Current Practices in Mobility*, *3*(2020-01-2021), 113–136.

Braun, M., Schröder, W., & Klaas, M. (2019). High-speed tomographic PIV measurements in a DISI engine. *Experiments in Fluids*, *60*, 1–26.

Choi, K.-S., & Lumley, J. L. (2001). The return to isotropy of homogeneous turbulence. *Journal of Fluid Mechanics*, *436*, 59–84.

Jiang, S., Campbell, D., Lu, Y., Li, H., & Hartley, R. (2021). Learning to estimate hidden motions with global motion aggregation. In *Proceedings of the IEEE/CVF international conference on computer vision* (pp. 9772–9781).

Jülich Supercomputing Centre. (2021). JUWELS Cluster and Booster: Exascale Pathfinder with Modular Supercomputing Architecture at Juelich Supercomputing Centre. *Journal of large-scale research facilities*, *7*(A138). doi: 10.17815/jlsrf-7-183

Lagemann, C., Lagemann, K., Mukherjee, S., & Schröder, W. (2021). Deep recurrent optical flow learning for particle image velocimetry data. *Nature Machine Intelligence*, *3*(7), 641–651.

Lagemann, C., Lagemann, K., Mukherjee, S., & Schröder, W. (2022). Generalization of deep recurrent optical flow estimation for particle-image velocimetry data. *Measurement Science and Technology*, *33*(9), 094003.

Lumley, J. L., & Newman, G. R. (1977). The return to isotropy of homogeneous turbulence. *Journal of Fluid Mechanics*, *82*(1), 161–178.

Marquardt, P., Klaas, M., & Schröder, W. (2019). Experimental investigation of isoenergetic film-cooling flows with shock interaction. *AIAA Journal*, *57*(9), 3910–3923.

Raffel, M., Willert, C. E., Scarano, F., Kähler, C. J., Wereley, S. T., & Kompenhans, J. (2018). *Particle image velocimetry: a Practical Guide*. springer.

Teed, Z., & Deng, J. (2020). Raft: Recurrent all-pairs field transforms for optical flow. In *Computer Vision–ECCV 2020: 16th European Conference, Glasgow, UK, August 23–28, 2020, Proceedings, Part II 16* (pp. 402–419).